Current Research in Environmental & Applied Mycology (Journal of Fungal Biology)
16(1): 257–275 (2026) ISSN 2229-2225
www.creamjournal.org **Article**
Doi 10.5943/cream/16/1/12

Beneficial traits of endolichenic fungi from *Usnea*: Antagonism against *Fusarium oxysporum* and growth promoting properties

Co RJO[1,2] and dela Cruz TEE[1,2,3*]

[1] The Graduate School, University of Santo Tomas, España Blvd. 1008 Manila, Philippines
[2] Fungal Biodiversity, Ecogenomics & Systematics-Metabolomics (FBeS) Group, Research Center for the Natural and Applied Sciences, University of Santo Tomas, España Blvd. 1008 Manila, Philippines
[3] Department of Biological Sciences, College of Science, University of Santo Tomas, España Blvd. 1008 Manila, Philippines

Co RJO, dela Cruz TEE 2026 – Beneficial traits of endolichenic fungi from *Usnea*: Antagonism against *Fusarium oxysporum* and growth promoting properties. Current Research in Environmental & Applied Mycology (Journal of Fungal Biology) 16(1), 257–275, Doi 10.5943/cream/16/1/12

Abstract

Plant growth-promoting (PGP) traits due to plant-associated microorganisms are crucial to enhance crop productivity and ensure sustainable agriculture. Endolichenic fungi (ELF), a unique group of fungal symbionts that inhabit healthy lichen tissues, share ecological similarities, and perhaps also roles with fungal endophytes in plants, and thus, can be tapped as bioinoculants like their fungal endophytic counterparts. Hence, of particular interest are the beneficial traits of ELF. In this study, we isolated forty ELF from the fruticose lichen *Usnea* and evaluated these for PGP traits, particularly on the production of indole-3-acetic acid (IAA), phosphate solubilization, and antagonistic activity against the pathogen *Fusarium oxysporum*. IAA production was assessed in liquid medium supplemented with L-trytophan. Our results showed 24 ELF isolates exhibiting IAA activity, with IAA concentration reaching up to 45 µg/mL. Among these ELF, *Xylaria enteroleuca* (SG5MB3) produced the highest with 45.9 ± 0.03 µg/mL of equivalent IAA. Phosphate solubilization was evaluated through agar-based assay using Pikovskaya's medium. Solubility index showed 24 ELF isolates which can solubilize insoluble phosphate, with indices of 2.10–2.92. Among these, *Hyphopichia wangnamkhiaoensis* (SG1MA2) and *Xylaria laevis* (SG4MB5.2) had the most notable phosphate solubilization. Assays for antagonistic activities showed that ELF inhibited *F. oxysporum* by up to 57%, with mutual inhibition upon mycelial contact being the most observed interaction between the test pathogen and the ELF. Our findings indicated multiple PGP traits by ELF, highlighting their potential as bioinoculants for sustainable crop production through IAA-mediated plant growth promotion, improved nutrient availability via phosphate solubilization, and the potential suppression of soil-borne pathogens through antagonistic activity.

Keywords – biocontrol – dual-culture – indole-3-acetic acid – phosphate solubility – sustainable agriculture

Introduction

Fungi are among the most diverse organisms, fulfilling ecological roles from decomposition to mutualism, and exhibit biotechnological importance. In animals, mycobiota can modulate immunity, aid nutrient acquisition, and provide protection against pathogens (Underhill & Iliev 2014, Sachdeva & Das 2022). Comparable benefits also occur in plants, where fungal symbionts enhance nutrient

Submitted 17 October 2025, Accepted 11 June 2026, Published 07 August 2026
Corresponding Author: Thomas Edison E. dela Cruz – e-mail – tedelacruz@ust.edu.ph

uptake, secrete phytohormones such as indole-3-acetic acid (IAA) and gibberellins, improve tolerance to abiotic stress, and antagonize pathogens through competition, antibiosis, or mycoparasitism (García-Latorre et al. 2023). These fungal traits not only drive ecosystem dynamics on land (Treseder & Lennon 2015) but have also been harnessed in the development of microbial inoculants. Examples of microbial-based inoculants use the soil fungus *Trichoderma*, mycorrhizal fungi, and rhizobia, which are established in sustainable farming systems to enhance plant growth and confer protection against disease (Schouteden et al. 2015, Guzmán-Guzmán et al. 2019, dela Cruz et al. 2023). These traits position fungal inoculants as sustainable alternatives to chemical fertilizers and pesticides.

Beyond the classical partnership between a mycobiont and a photobiont, lichens are known to harbor diverse microbial associates, including bacteria, yeasts, and other filamentous fungi (Grimm et al. 2021). Among these filamentous fungi are the ELF, which colonize healthy lichen thalli internally without causing disease and have been described as analogs to fungal endophytes in plants. ELF maintain stable associations with their host lichens and may harbor similar traits of biocontrol with that of fungal endophytes, though their ecological functions remain understudied (U'Ren et al. 2012, Suryanarayanan & Thirunavukkarasu 2017).

Most investigations on ELF have focused on their secondary metabolites, many of which display antimicrobial, anticancer, or antioxidant activities (Kellogg & Raja 2017, Zhang et al. 2024). Others have documented their phylogenetic diversity and enzymatic capacity to thrive in high-altitude areas and extreme microenvironments (Grimm et al. 2021, Wang et al. 2022, Li et al. 2023). The Philippines, with its rich lichen diversity documented across multiple regions, and its tropical climate that supports abundant lichen communities, represents a promising frontier for the study of ELF (Paguirigan et al. 2020, Taer et al. 2023). Its diverse ecosystems provide numerous lichen hosts, making it an ideal setting for isolating and characterizing ELF. Among the recent studies that explored ELF in the country have focused on the diversity and bioactivities of *Ramalina*, *Usnea*, and *Parmotrema*, revealing their potential as sources of novel compounds with pharmaceutical and agricultural value. From *Usnea* species, 101 ELF isolates belonging to 12 genera were identified, of which *Nemania* (50.5%) and *Xylaria* (22.8%) were the dominant taxa. Their culture extracts showed broad antimicrobial and antioxidant activities, often stronger than those of the lichen host (Santiago et al. 2021). ELF from *Ramalina* and *Usnea* also exhibited great inhibition against *Colletotrichum gloeosporioides, Cladosporium cladosporioides,* and *Fusarium oxysporum* (Jamilano-Llames & dela Cruz 2025). Similarly, ELF from *Ramalina peruviana*, including *Colletotrichum, Daldinia, Hypoxylon, Nemania, Nigrospora,* and *Xylaria*, displayed high radical scavenging activity, suggesting a protective role in the lichen symbiosis (Galinato et al. 2021). ELF isolated from *Parmotrema rampoddense* also showed antibacterial activity against ESKAPE pathogens, with *Fusarium proliferatum* (Tan et al. 2020) and *Cubamyces menziesii* (Tan et al. 2024) producing potent inhibition and antimicrobial compounds.

However, despite the growing evidence of ELF bioactivity, their functional roles in plants and agriculture remain poorly understood. In contrast, fungal endophytes have been widely studied for their beneficial traits, such as plant growth promotion (Cruz & dela Cruz 2024) and plant protection against pathogens (Huang et al. 2024). Since lichens are known to thrive in extreme environments where few organisms can survive, their associated ELF may contribute to this resilience by producing growth-stimulating hormones and exhibiting antagonistic activity against competing microorganisms. Similar interactions have been observed in lichen symbioses, where associated microbial partners enhance host adaptation and metabolic stability under stress (Grube et al. 2015), and in endophyte–host systems that improve plant tolerance and defense mechanisms (Karunasinghe et al. 2020).

Given this, it is reasonable to examine whether ELF possess functional traits commonly associated with plant growth-promoting fungi, particularly phytohormone production, nutrient mobilization, and pathogen suppression. Evaluating these traits provides insight into both their ecological role within lichens and their potential application in sustainable agriculture. Thus, this study investigated the growth-promoting and antagonistic properties of ELF isolated from the young

and mature thalli of the fruticose lichen *Usnea*. Growth promotion was assessed through indole-3-acetic acid (IAA) production and phosphate solubilization, while protection was evaluated based on the ability of ELF to inhibit the fungal pathogen *Fusarium oxysporum*. We hypothesized that ELF isolates derived from mature thalli, having a more established relationship with their host lichen, exhibited better beneficial traits to aid their lichen host, than those isolated from young thalli.

Materials & Methods

Sample collection and isolation

Lichen thalli were collected in Sagada, Mountain Province, located in northern Philippines. This highland municipality in the Cordillera Mountain Range is characterized by pine-dominated forests and a cool climate ranging from 10–15°C at night to 20–25°C during the day. Young (thallus length: 2.9±1.5 cm, equivalent to 5 to 7 years) and mature (thallus length: 6.6±1.7cm, equivalent to 12 to 15 years) thalli of *Usnea* (n = 10) were collected from five sites: Brgy. Bangaan (17°07'09.4"N, 120°53'48.8"E & 17°05'50.4"N, 120°54'26.2"E), Brgy. Antadao (17°04′25.6″ N, 120°55′32.0″ E), and Brgy. Patay (17°04′55.4″ N, 120°54′11.9″ E & 17°05′02.7″ N, 120°54′20.2″ E). Each site yielded one young and one mature thallus, designated as SG1Y/M through SG5Y/M. The age of the lichen thalli was estimated by dividing the thallus length (mm) to lichen growth rate (mm/year) following the protocol of Li et al. (2014), which was based on the growth rates (4.3 to 5.5 mm per year) of *Usnea aurantiacoatra*. Isolation of ELF followed a modified method of Maduranga et al. (2018). Lichen thalli were rinsed, cut into 1–2 cm² fragments, and surface sterilized sequentially in 70% ethanol (90 s), 0.5% sodium hypochlorite (3 min), and 70% ethanol (90 s), followed by three rinses in sterile distilled water. Sterilized fragments were blotted dry on sterile filter paper, plated on Dichloran Rose Bengal Chloramphenicol Agar (DRBCA; HiMedia, India), and incubated at room temperature for 14 days. Sterilization efficacy was verified using tissue imprint controls on agar. Emerging hyphae were sub-cultured on Potato Dextrose Agar (PDA; TM Media, India) and assigned strain codes. A total of 148 ELF isolates, designated here as Sagada-ELF, were obtained. From these, 40 representative ELF isolates were selected based on distinct colonial morphology and thallus origin, that is, isolates were uniquely associated with young thalli (n= 10), mature thalli (n = 10), and those occurring in both thallus types (n = 20).

Assessment of beneficial traits

Antagonistic activity against Fusarium oxysporum

The antagonistic activity of ELF isolates against *F. oxysporum* was evaluated using a dual-culture assay adapted from Jamilano-Llames & dela Cruz (2025). A 5-mm mycelial plug from a 7-day-old culture of *F. oxysporum* was placed 15 mm from the edge of a PDA plate opposite a 5-mm plug of a 7-day-old ELF isolate. Control plates containing either the pathogen or the ELF alone were included. Plates were sealed and incubated at room temperature for 10 days. Pathogen growth was measured daily along the axis facing the ELF (r_2) and away from the ELF (r_1). The percentage inhibition of pathogen growth was calculated as:

$$\%\ inhibition\ =\ (\frac{r1-r2}{r1})x100$$

Each assay was performed in triplicates. Mycelial interactions were also assessed on day 10 following Wicklow's (1975) classification: Type A (intermingling with no inhibition), Type B (mutual inhibition with clear zone), Type C (mutual inhibition at a distance), Type D (unilateral inhibition at contact), and Type E (unilateral inhibition at a distance with a clear inhibition zone).

Phosphate solubility plate assay

Phosphate solubilization (PS) was assessed on Pikovskaya's agar (PVK) following the protocol of Cruz & dela Cruz (2024). A 5-mm mycelial plug from a 7-day-old ELF culture was inoculated at

the center of PVK plates; uninoculated plates served as controls. Each isolate was tested in triplicates. Plates were incubated at 28 ± 2°C for 7 d in the dark, after which halo formation was recorded. Colony diameter (CD) and clear zone diameter (CZD; colony + halo) were measured along two perpendicular axes and averaged. Solubilization Index (SI) and Solubilization Efficiency (SE) were calculated as:

$$SI = \frac{Colony\ Diameter\ (CD) + Halo\ Diameter\ (CZD)}{Colony\ Diameter\ (CD)}$$

$$SE\ (\%) = \frac{CZD - CD}{CD}\ x\ 100$$

Isolates were further categorized based on the clarity of the halo as non-PS (n-PS, no halo observed or no phosphate solubilization), fair PS (f-PS, with faint or hazy halo surrounding the colony), or good PS (g-PS, with clear halo surrounding the colony).

Indole-3-Acetic Acid (IAA) production assay

ELF isolates were inoculated into 40mL Czapek-Dox broth (CDB) supplemented with 0.1% (w/v) L-tryptophan and incubated at 28°C, 150 rpm for 10 d in the dark. Cultures were then centrifuged (10,000 × g, 10 min), and 100 µL of the supernatant was mixed with 200 µL of Salkowski's reagent. The mixtures were incubated at room temperature for 30 min in the dark. Development of a pink to reddish color indicated IAA production, while uninoculated broth served as a control. For quantification, absorbance was measured at 530 nm using a UV–Vis spectrophotometer (Spectrostar nano, BMG Labtech, USA). IAA concentration (µg/mL) was determined from a standard curve prepared with pure IAA (Sigma-Aldrich, USA) in the range of 5–100 µg/mL. Each isolate was assayed in triplicates, and results are expressed as mean ± SD.

Data analysis

Data was analyzed statistically using one-way Analysis of Variance (ANOVA). As a post hoc test, the significant differences in the computed mean values were compared by student t-test and Levene's test at $p \leq 0.05$.

Molecular identification and phylogenetic analysis

Ten good-performing beneficial ELF were then subjected to molecular characterization and phylogenetic analysis to confirm species identities. Extraction, purification, PCR amplification, and sequencing were performed as outsource service by Macrogen, South Korea. We sequenced the internal transcribed spacer (ITS) region of rRNA genes using the primer pairs ITS5F (5'-GGAAGTAAAAGTCGTAACAAGG-3') and ITS4R (5'-TCCTCCGCTTATTGATATGC-3'). Forward and reverse ITS sequences were then assembled into consensus contigs using CodonCode Aligner (v. 9.0.1; CodonCode Corporation, Centerville, MA, USA). Low-quality regions and ambiguous bases were manually trimmed, and high-quality sequences were exported in FASTA format. Sequence comparison was carried out through BLAST search to identify generic affiliation. For phylogenetic analysis, reference sequences were retrieved from published literature to construct a backbone tree. Sequences were aligned and curated with BMGE using NGPhylogeny.fr (Lemoine et al. 2019). Maximum likelihood analysis was performed with RAxML-HPC (GTR+G model, 1000 bootstrap replicates) via the CIPRES Science Gateway (Miller et al. 2011). The best-scoring tree was visualized and annotated in FigTree (Rambaut 2009).

Results

Of the 40 Sagada-ELF isolates chosen for this study, 20 originated from young *Usnea* thalli and 20 from mature *Usnea* thalli. Ten were isolated only from young, another ten from mature, and 20 with similar colonial morphologies were observed in both young and mature thalli.

Antagonism against Fusarium oxysporum

Dual-culture assays revealed that Sagada-ELF isolates from both young (Y) and mature (M) *Usnea* thalli exhibited varying levels of antagonistic activity against *F. oxysporum* (Fig. 1). Percent growth inhibition of the pathogen by Sagada-ELF ranged from 5.18% to 58.96%, while inhibition of ELF by the pathogen ranged from 10.61% to 83.24%. Among the young thallus Sagada ELF isolates, SG1YD1 exhibited the highest inhibition of *F. oxysporum* (58.96 ± 1.50%), followed by SG5YD3 (49.19 ± 1.39%), SG1YA1 (46.45 ± 2.62%) and SG3YA2 (41.32 ± 0.95%). Other young thallus Sagada ELF isolates such as SG1YB4, SG1YB2, and SG3YD4.1 also showed moderate inhibition values ranging from 37–40%. For isolates obtained from mature thalli, the highest inhibition was observed in SG5MA1.2 (47.28 ± 1.88%), and SG5MB3.1 (46.38 ± 1.37%). Several other mature thalli Sagada ELF isolates, including SG2MB1, SG5MA3, and SG4MB5.2, also produced inhibition levels between 40–44%, while SG5MC5 exhibited the lowest inhibition value (5.18 ± 2.93%). When grouped by developmental stage, Sagada-ELF isolates from young *Usnea* thalli had inhibition values ranging from 19.68% to 58.96%, while Sagada-ELF isolates from mature *Usnea* thalli ranged from 5.18% to 49.19%. However, the mean percent inhibition of *F. oxysporum* by Sagada-ELF from young thalli (36.1 ± 10.1%) did not significantly differ from those obtained from mature thalli (35.5 ± 10.8%) (t-test, $p > 0.05$). Variability between the two groups was also not significantly different (Levene's test, $p > 0.05$), suggesting that both groups exhibited similar levels of antagonistic activity.

The growth of *F. oxysporum* in dual culture with Sagada-ELF was monitored for ten days and evaluated for the type of interaction (Fig. 2). In the control plates, that is, unopposed *F. oxysporum* and unopposed Sagada-ELF, the pathogen and the ELF isolates showed continuous, progressive colony expansion and unimpeded growth, mostly reaching the highest colony diameter by day 10. In dual cultures, the pathogen's growth was generally slower compared to the control (unopposed *F. oxysporum*), although there were 11 Sagada-ELF from young thalli and 8 Sagada-ELF from mature thalli that were inhibited by the pathogen (Fig. 1). A wider spread of growth trajectories was noted among isolates from young thalli, indicating greater variability in pathogen suppression compared with those from mature thalli. Interestingly, three Sagada-ELF (SG1YD2, SG1YB2, SG1YA1) from young thalli and five Sagada-ELF (SG1MA2, SG2MB3, SG1MB4, SG5MA1.2, SG5MB3) from mature thalli greatly inhibited the pathogen.

Among the Sagada-ELF isolates, Type B was the most common type of interaction, which was observed in 18 isolates (7 from young, 11 from mature thalli). Both the pathogen and the ELF exhibited mutual inhibition upon contact (Fig. 2). Type D, inhibition of one fungus by the other upon contact, was recorded among 9 Sagada-ELF isolates (6 from young, 3 from mature) while Type E, inhibition of one fungus by the other at a distance, occurred in 8 isolates (3 from young and 5 from mature). Type C whereas one fungus is clearly inhibited by the other fungus was identified in 4 Sagada-ELF isolates (3 from young, 1 from mature). Type A, the least frequent, was observed in only one Sagada-ELF isolate and these showed mutual intermingling with the pathogen. Sagada-ELF isolates from both young and mature thalli exhibited all five interaction types. ELF isolates from young *Usnea* thalli showed a higher number of Type D interactions, while ELF isolates from mature *Usnea* thalli had a greater number of Type B and Type E interactions.

Phosphate solubilization

We used agar-based method with Pikovkaya's agar to test the ability of Sagada-ELF to solubilize phosphate (Fig. 3). A distinct and clear zones or halo surrounding fungal colonies indicates solubilization of phosphates present in the medium as observed in 24 Sagada-ELF. We also observed faint or hazy dissolution of phosphates in the agar plates by 11 Sagada-ELF isolates indicating partial solubilization. Now, the Sagada-ELF isolates from the young and mature thalli of *Usnea* exhibited variable phosphate solubilization capabilities, as reflected in their solubility index (SI) and solubilization efficiency (SE) values (Table 1). Among ELF isolates derived from mature thalli, the phosphate solubility index ranged from 2.11 ± 0.04 to 2.94 ± 0.73, with the highest recorded in SG4MA5 (2.94 ± 0.73) and SG4MB5.2 (2.92 ± 0.73). Correspondingly, phosphate solubilization

efficiency (SE) in these ELF isolates ranged between 9.82 ± 1.97% and 92.18 ± 5.98%, with SG4MA5 and SG4MB5.2 also showing the highest SE values.

For Sagada-ELF isolates obtained from young thalli, SI values ranged from 2.10 ± 0.08 to 2.34 ± 0.09, while SE ranged between 15.22 ± 4.73% and 35.39 ± 1.91%. The highest phosphate solubilization activity among ELF isolates from this thallus type was recorded in SG2YA5 (SI = 2.34 ± 0.09; SE = 32.58 ± 9.43%) and SG1YD1 (SI = 2.24 ± 0.08; SE = 30.37 ± 4.67%). Overall, Sagada-ELF isolates from mature *Usnea* displayed higher phosphate solubilization efficiency, with several isolates achieving SE values above 90%, than Sagada-ELF isolates from young thalli, which generally showed moderate solubilization (up to 35%).

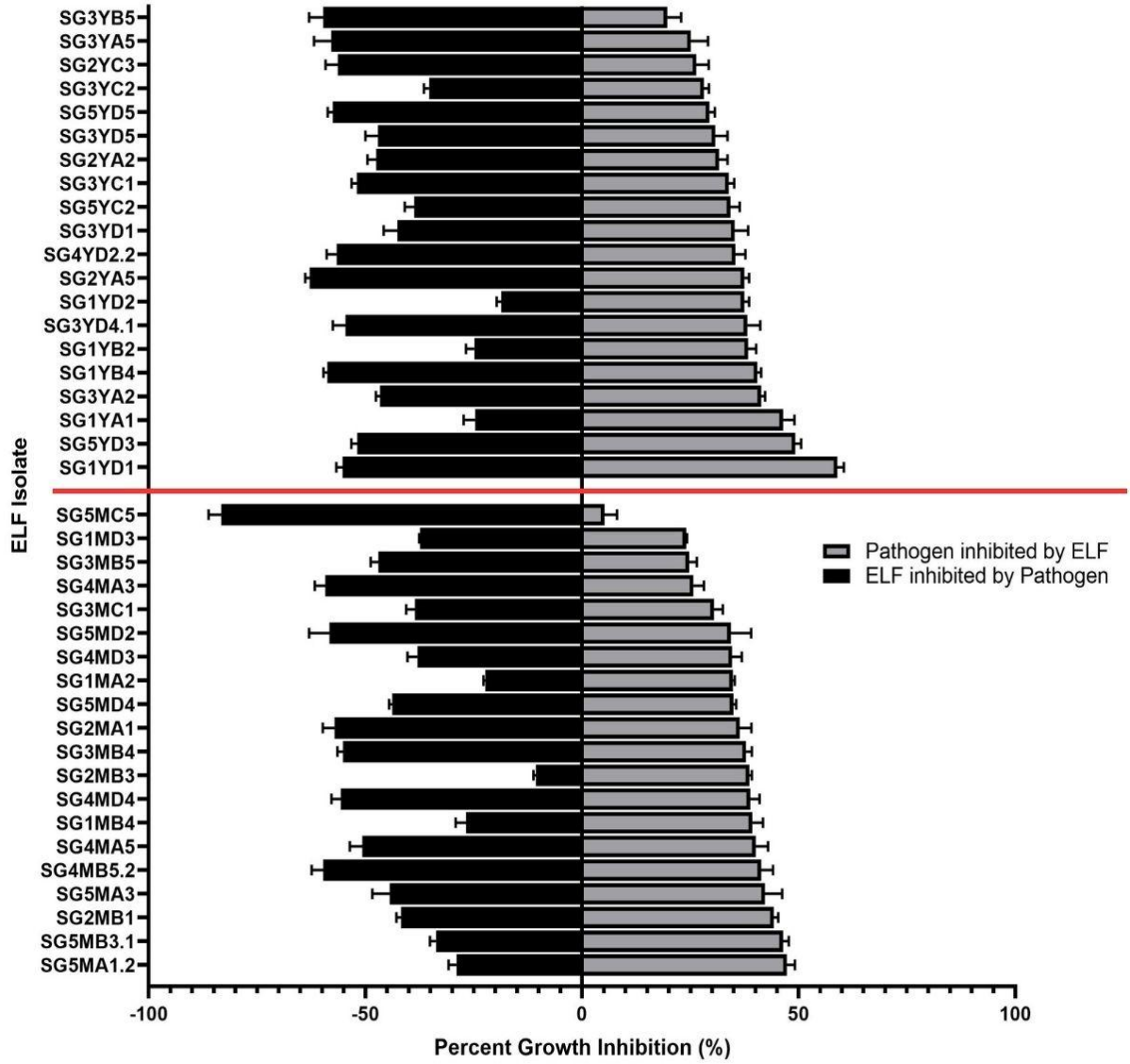

Fig. 1 – Antagonism between ELF and *F. oxysporum* on the 10th day of interaction. Isolates are arranged according to the degree to which the pathogen was inhibited by each ELF. Bars represent mean percent growth inhibition (±SD, n = 3). ELF isolates above the red line are Sagada-ELF obtained from young *Usnea* thalli, while those below are from mature *Usnea* thalli.

Fig. 4 illustrates the IAA production and PSI of ELF from different thallus ages. Both parameters varied across isolates, reflecting functional diversity among the ELF community. IAA production among the ELF isolates ranged from 7.89 to 45.89 µg/mL, PSI were between 2.11 and 2.92. The highest IAA concentrations were recorded in mature thallus isolates, particularly

SG5MB3.1 (*Xylaria berteroi*) and SG4MB5.2 (*Xylaria laevis*), which produced 45.89 ± 3.29 µg/mL and 41.38 ± 2.15 µg/mL, respectively.

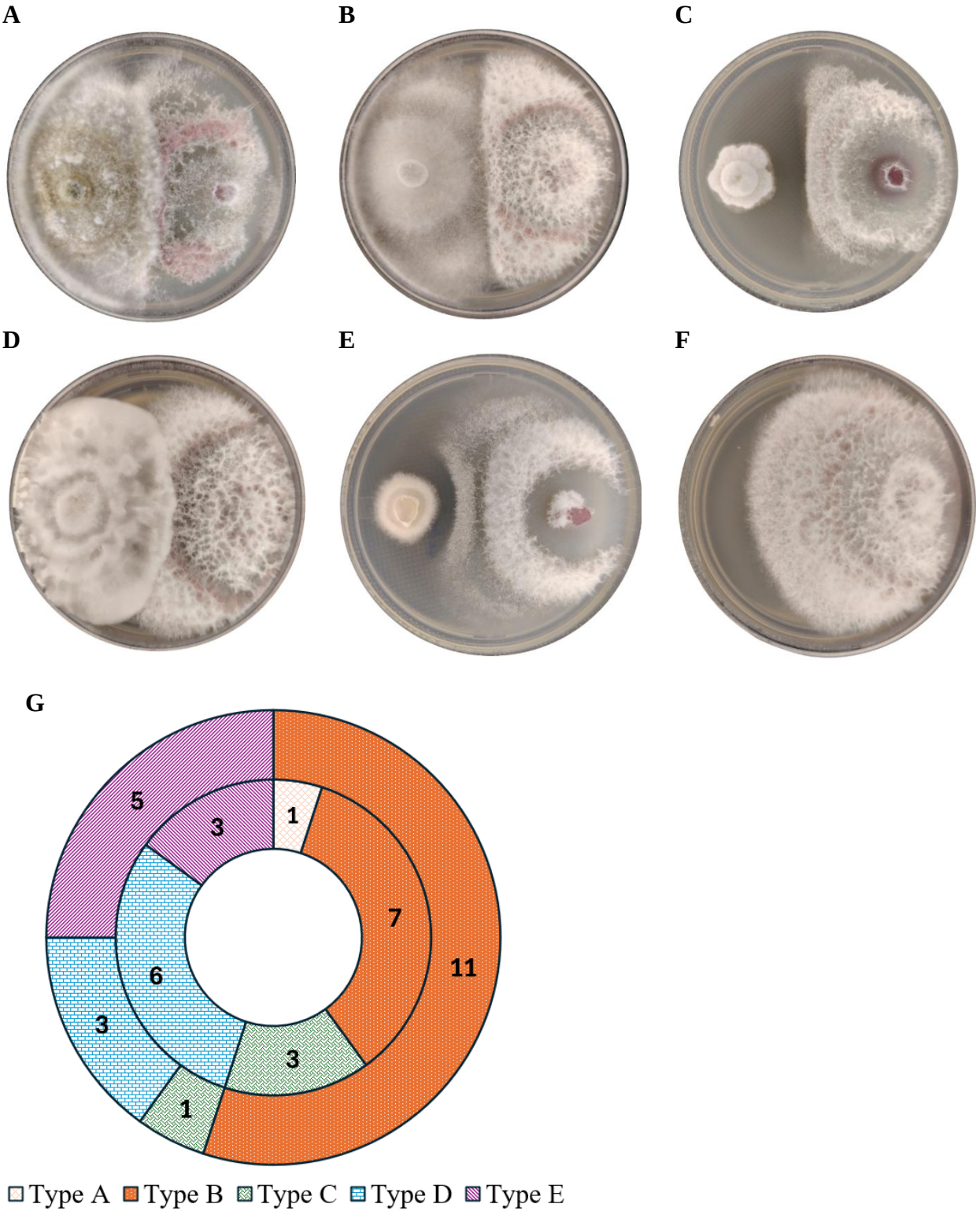

Fig. 2 – Growth of *F. oxysporum* in dual culture with Sagada-ELF from young and mature *Usnea* thalli over a 10-day incubation period: *Fusarium oxysporum* (right side of each plate), ELF isolates (left side). Each plate (A–F) illustrates a representative type of antagonism observed in the study. (**A)** SG4MD4. (**B**) SG1YA1. (**C**) SG1YB2. (**D**) SG5MA1.2. (**E)** SG3YC2. (**F**) unopposed *F. oxysporum* (control). (**G**) Distribution of antagonistic interaction types among ELF isolates from young (outer ring) and mature (inner ring) *Usnea* thalli.

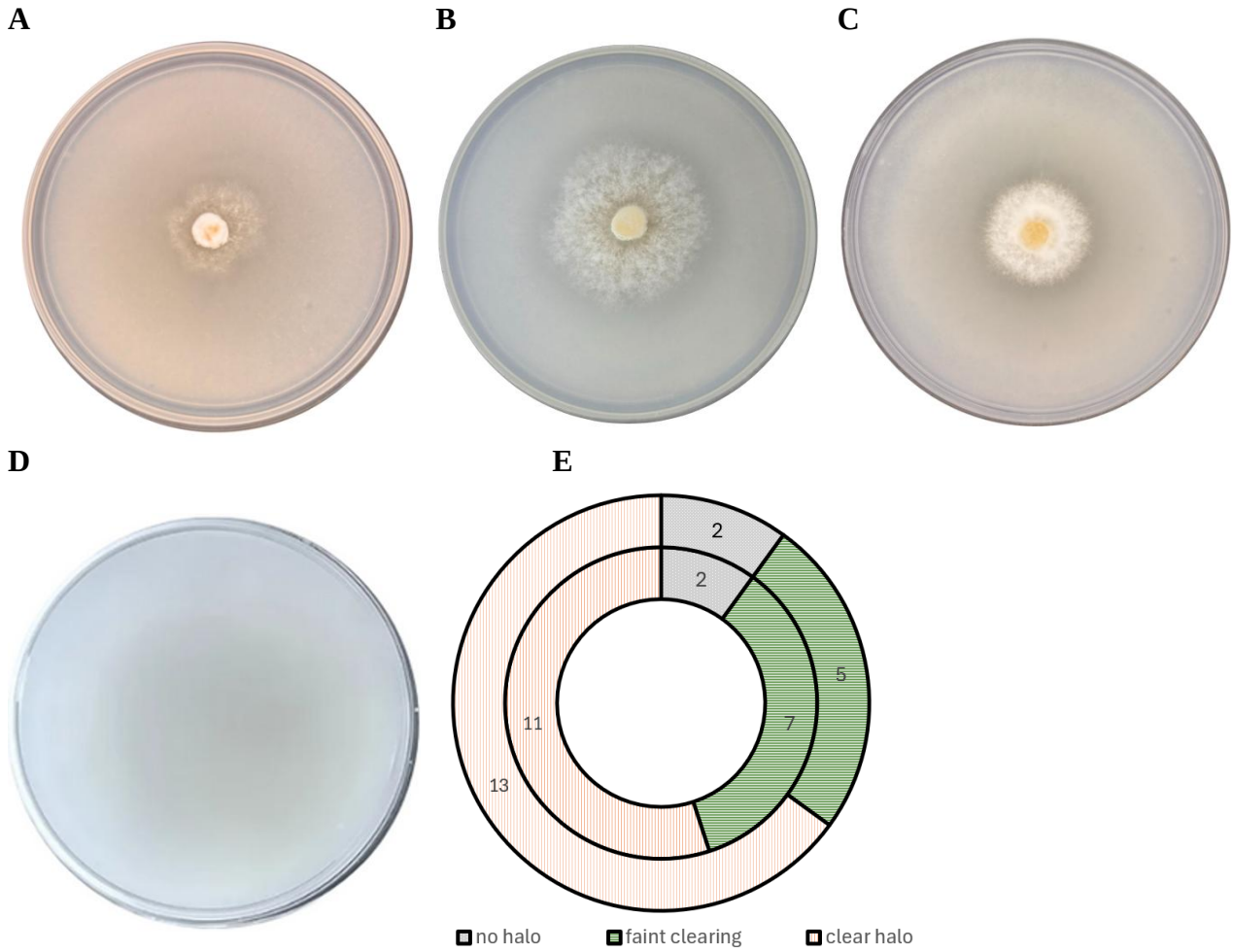

Fig. 3 – Phosphate solubilization of Sagada-ELF isolates using Pikovkaya's Agar indicating clear zone around fungal colony. Each plate (A–C) represents an isolate producing no halo (SG2MB3), faint clearing (SG3YA5) and clear halo around fungal colony (SG3MC1), with uninoculated PKV agar (D). The number of Sagada-ELF isolates from young (outer ring) and mature (inner ring) *Usnea* thalli exhibiting different levels of phosphate solubilization is presented in E.

IAA production

Similarly, IAA production varied widely among and between the Sagada-ELF isolates obtained from the two thallus types. ELF isolates from mature thalli produced IAA in concentrations ranging from 1.34 ± 0.61 to 45.89 ± 9.23 µg/mL, with SG5MB3 (45.89 ± 9.23 µg/mL), SG4MA3 (31.64 ± 9.91 µg/mL), and SG5MD4 (30.34 ± 9.08 µg/mL) showing the highest production levels. In comparison, ELF isolates from young thalli produced IAA within a range of 0.72 ± 0.06 to 38.74 ± 7.96 µg/mL. The highest IAA-producing ELF isolates from this group were SG5YD5 (38.74 ± 7.96 µg/mL), SG3YD4.1 (31.9 ± 1.63 µg/mL), and SG2YD2 (18.65 ± 6.04 µg/mL). When grouped, mean IAA levels were comparable between ELF isolates from young and mature thalli, though individual mature isolates exhibited higher maximum values. Both groups contained strains capable of producing >30 µg/mL of IAA, indicating strong potential for plant growth promotion regardless of developmental stage.

Both also exhibited relatively high PSI values (2.31 ± 0.03 and 2.92 ± 0.73, respectively), suggesting strong dual growth–promoting potential. In contrast, young thallus isolates such as SG1YB4 *(Fusarium incarnatum*) and SG2YA2 (*Fusarium equiseti*) showed the lowest IAA levels (7.89 ± 0.08 µg/mL and 9.56 ± 7.89 µg/mL, respectively), although their PSI values (2.22 ± 0.03 and 2.33 ± 0.09) remained comparable to those of mature isolates.

Table 1 Type of antagonistic interaction, quantitative analysis of IAA production and phosphate solubilization activity of ELF isolates.

Isolate Code[a]	Type of Interaction[b]	Phosphate solubility index[c]	Phosphate solubility efficiency (%)[c]	Production of Indole3-acetic acid (µg/mL)[d]
SG1MA2	**Type B**	**2.11±0.04**	**11.12±3.89**	**27.41±0.79**
SG1MB4	Type D	-	-	-
SG1MD3	**Type D**	**2.17±0.01**	**17.21±1.19**	**15.45±2.51**
SG2MA1	Type B	-	-	-
SG2MB1	Type D	2.21±0.07	20.78±6.52	-
SG2MB3	Type C	-	-	1.34±0.61
SG3MB4	Type E	-	-	6.23±1.18
SG3MB5	Type E	2.26±0.06	26.36±6.28	-
SG3MC1	Type B	2.1±0.02	9.82±1.97	-
SG4MA3	**Type B**	**2.28±0.04**	**27.83±4.08**	**31.64±9.91**
SG4MA5	Type E	2.54±0.35	53.77±3.91	-
SG4MB5.2	**Type B**	**2.92±0.73**	**92.18±5.98**	**21.02±3.02**
SG4MD3	Type C	-	-	32.59±8.17
SG4MD4	Type A	-	-	-
SG4YD2.2	Type B	-	-	
SG5MA1.2	Type D	2.92±0.73	92.18±7.27	0.28±1.52
SG5MA3	Type D	-	-	19.29±1.95
SG5MB3.1	**Type D**	**2.19±0.04**	**19.34±4.28**	**45.89±3.29**
SG5MC5	**Type C**	**2.31±0.03**	**30.63±3.2**	**11.16±3.48**
SG5MD2	Type B	2.15±0.03	15.37±3.18	-
SG5MD4	**Type B**	**2.37±0.37**	**37.1±6.99**	**30.34±9.08**
SG1YA1	Type D	-	-	-
SG1YB2	Type C	-	-	4.39±0.44
SG1YB4	**Type E**	**2.22±0.03**	**21.56±2.8**	**7.89±3.17**
SG1YD1	Type B	-	-	0.72±0.08
SG1YD2	Type B	2.24±0.08	23.58±7.91	1.57±0.48
SG2YA2	**Type E**	**2.33±0.09**	**32.58±9.43**	**9.56±7.89**
SG2YA5	Type B	-	-	15.51±1.23
SG2YC3	Type B	-	-	-
SG3YA2	Type B	2.26±0.07	26.2±7.05	-
SG3YA5	Type B	-	-	5.75±10.2
SG3YB5	Type D	-	-	-
SG3YC1	**Type B**	**2.27±0.07**	**27.1±6.58**	**19.12±0.62**
SG3YC2	Type E	2.15±0.05	15.22±4.73	-
SG3YD1	Type B	2.24±0.05	23.64±4.67	-
SG3YD4.1	Type E	2.3±0.16	30.37±16	3.91±6.13
SG3YD5	Type D	±	-	-
SG5YC2	**Type E**	**2.26±0.05**	**25.65±5.14**	**18.65±0.4**
SG5YD3	Type B	2.17±0.1	17.44±9.95	-
SG5YD5	**Type B**	**2.16±0.03**	**16.15±2.71**	**38.74±7.96**

Values are presented as mean ± SD (standard deviation); n = 3. Sagada-ELF isolates in BOLD denotes fungi with good growth promoting traits as shown in phosphate solubility (PSI > 2.0, PSE > 10%) and production of indole-3-acetic acid (> 5 µg/mL).

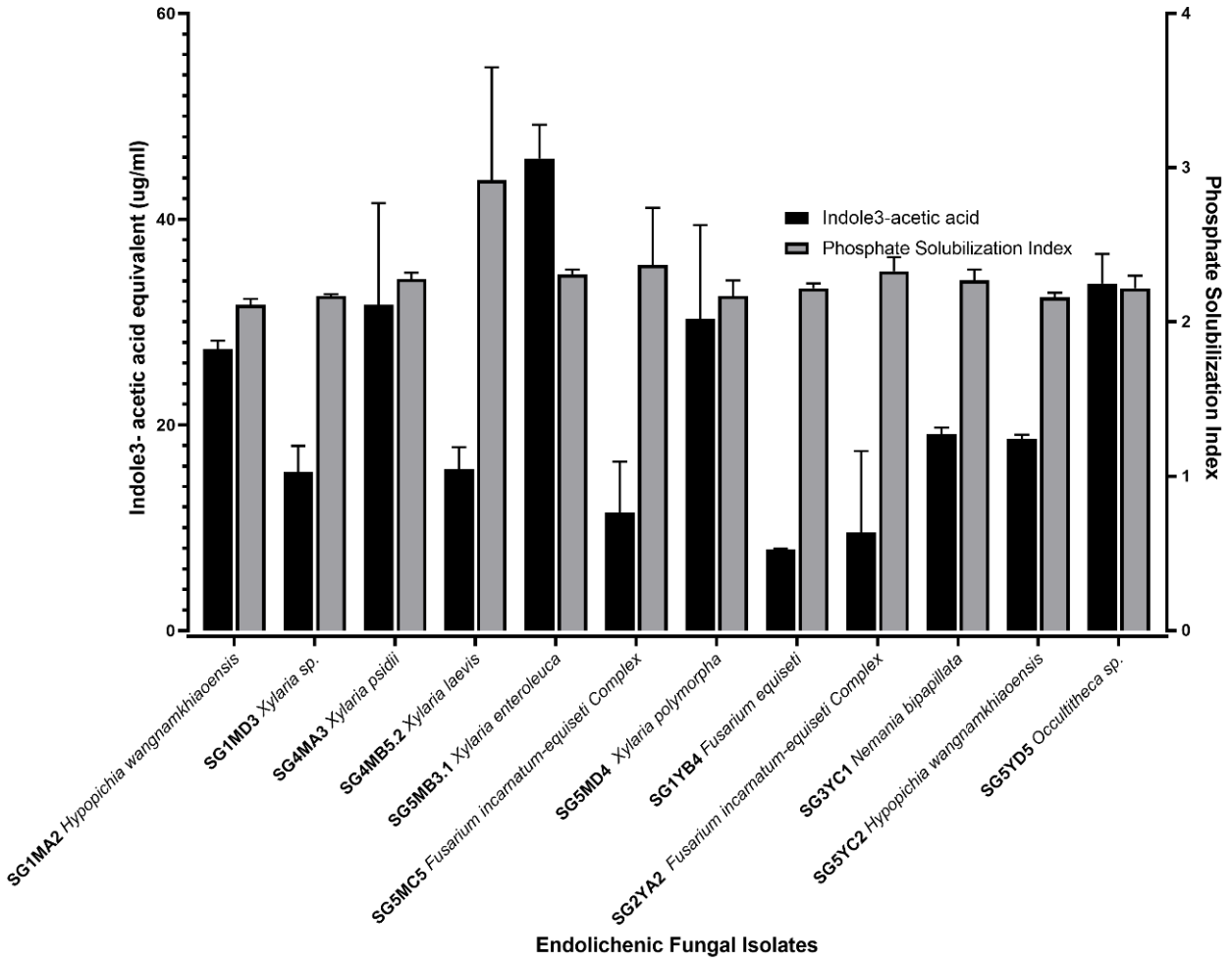

Fig. 4 – Indole-3-acetic acid (IAA) production and phosphate solubilization index of promising Sagada-ELF from young and mature *Usnea* thalli. Bars represent mean ± SD (n = 3).

Molecular identification

To complement the previous morphological observations, molecular identification based on ITS rDNA sequencing was carried out. In particular, the top-performing ELF isolates, as determined by their clear zone diameters and solubilization indices, were subjected to further molecular analysis using primers ITS4 and ITS5 to confirm their taxonomic placement.

Fig. 5 showed that the isolate formed a strongly supported clade (bootstrap = 89) with *Hyphopichia wangnamkhiaoensis* (MG969794, NR155178), indicating a close evolutionary relationship and suggesting that the isolate represents either a strain of *H. wangnamkhiaoensis* or a closely related taxon. The high bootstrap value supports its monophyly and stable placement within this lineage.

The overall topology of the tree corresponds well with established phylogenetic frameworks of *Hyphopichia*, which separate the genus from related yeasts such as *Meyerozyma* and *Debaryomyces*. Several *Hyphopichia* species, including *H. heimii*, *H. burtonii*, and *H. rhagii*, were recovered as distinct yet closely allied clades, reflecting the genus' narrow but well-differentiated taxonomic boundaries. The inclusion of multiple *Hyphopichia* type sequences and the strong bootstrap support for interspecific nodes affirm the phylogenetic integrity of the genus. Overall, the ITS-based analysis provides strong preliminary evidence that USTFBS SG5YC2 belongs to *Hyphopichia wangnamkhiaoensis* or a closely related species within the same clade.

The ITS-based phylogenetic analysis revealed that all five isolates (USTFBS_SG1MD3, USTFBS_SG4MA3, USTFBS_SG5MB3, USTFBS_SG4MB5.2, and USTFBS_SG5MD4) grouped within the genus *Xylaria* (family Xylariaceae, order Xylariales), forming well-supported clades with

known reference sequences (Fig. 6). The topology of the tree recovered several subclades consistent with those reported by Hsieh et al. (2010) and Daranagama et al. (2018), confirming the reliability of the reconstruction.

Fig. 5 – Maximum Likelihood phylogenetic tree based on ITS rDNA sequences showing the placement of isolate USTFBS_SG5YC2 within the genus *Hyphopichia*. Bootstrap values (>50%) from 1,000 replicates are shown at branch nodes. The tree was rooted using *Meyerozyma guilliermondii* (AY939792) and *Debaryomyces hansenii* (EU816290) as outgroups. Scale bar represents 0.08 substitutions per site.

Isolate USTFBS_SG1MD3 clustered with *X. atrodivaricata* (EU178739) and *X. griseosepiacea* (EU179865) with moderate bootstrap support, indicating affinity with the *X. atrodivaricata* lineage. USTFBS_SG4MA3 formed a strongly supported subclade (bootstrap = 100) with *X. psidii* (MT507833) and *X. palmicola* (GU322436), suggesting a close relationship to these tropical wood-inhabiting species. USTFBS_SG5MB3 grouped with *X. enteroleuca* (MH864898) and *X. berteroi* (GU324749) with high support (bootstrap = 84–88), while USTFBS_SG4MB5.2 clustered with *X. laevis* (KC771466). Lastly, USTFBS_SG5MD4 nested within a strongly supported clade (bootstrap = 100) containing *X. polymorpha* (FM164944, GU322460). The high bootstrap values for most nodes confirm stable phylogenetic placement, while minor unresolved internodes likely reflect the limited discriminatory power of ITS among closely related *Xylaria* taxa.

The phylogenetic analysis based on ITS sequences revealed that isolate USTFBS_SG3YC1 clustered within the genus *Nemania*, a member of the family Xylariaceae (Xylariales, Ascomycota). The isolate formed a strongly supported subclade (bootstrap = 100) with *Nemania bipapillata* (MH370736, GU292818), indicating a very close genetic relationship and suggesting that the isolate represents or is closely allied to *N. bipapillata* (Fig. 7). The high bootstrap value at this node provides strong evidence for monophyly and stable placement within this species lineage.

Overall, the strong phylogenetic affinity of USTFBS_SG3YC1 to *N. bipapillata* supports its preliminary identification as a member of this species, or at least as a closely related taxon within the *Nemania* clade. This placement expands the ecological spectrum of *Nemania*, which is typically wood-inhabiting, to include a lichen-associated endolichenic niche. Such associations highlight the ecological versatility of Xylariaceous fungi and their potential roles in decomposer and symbiotic networks.

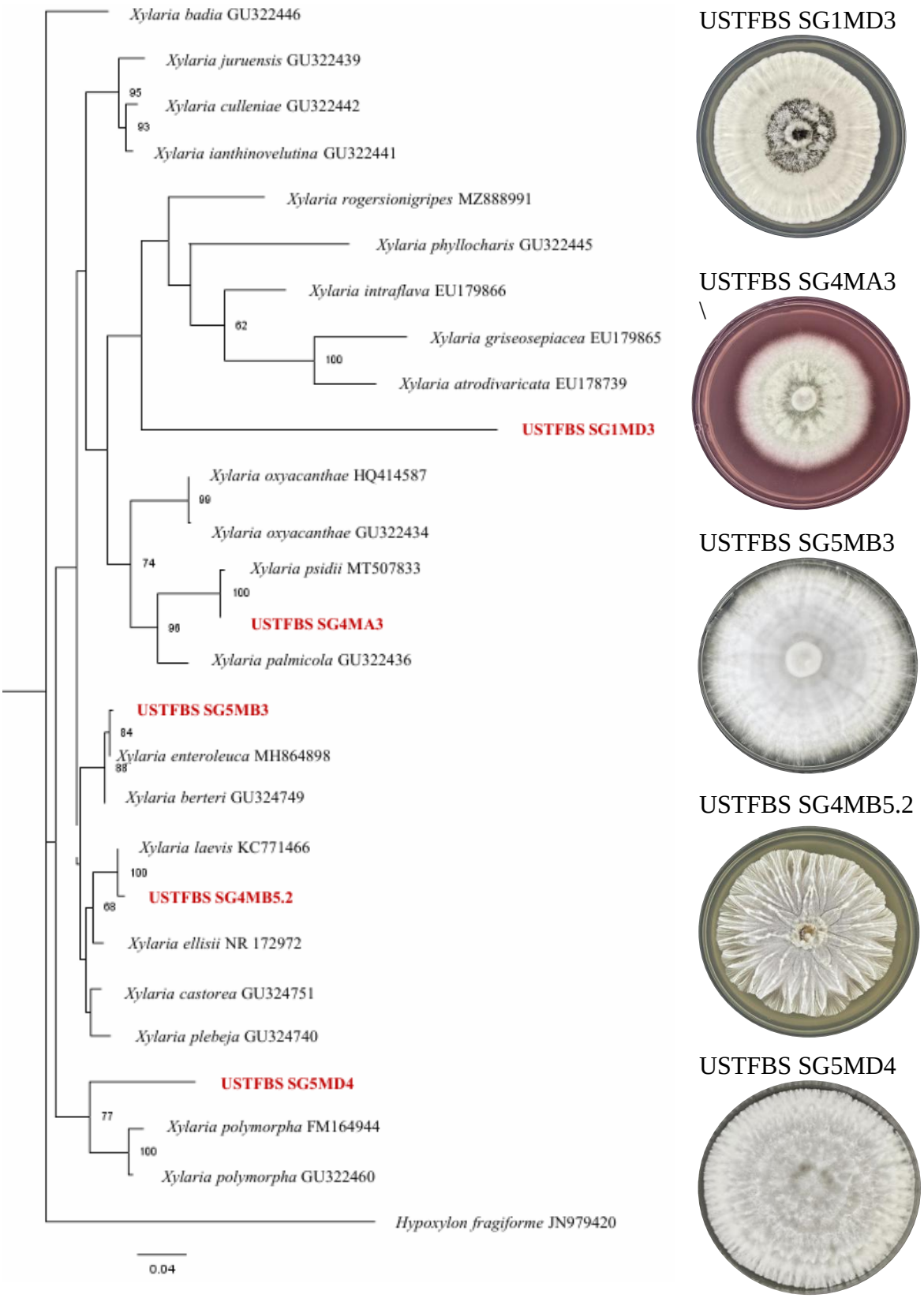

Fig. 6 – Maximum Likelihood phylogenetic tree based on ITS rDNA sequences showing the placement of ELF isolates USTFBS_SG1MD3, USTFBS_SG4MA3, USTFBS_SG5MB3, USTFBS_SG4MB5.2, and USTFBS_SG5MD4 within the genus *Xylaria*. Bootstrap values (>50%) from 1,000 replicates are shown at branch nodes. The tree was rooted using *Hypoxylon fragiforme* (JN979420) as outgroup. Scale bar represents 0.04 substitutions per site.

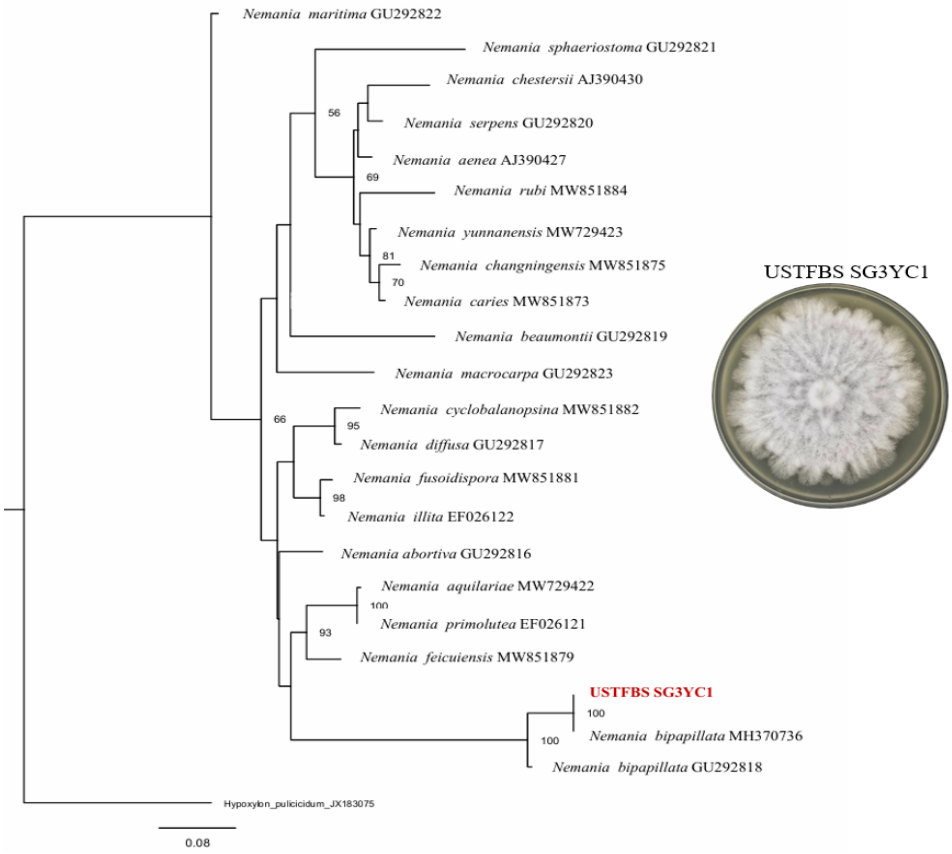

Fig. 7 – Maximum Likelihood phylogenetic tree based on ITS rDNA sequences showing the placement of isolate USTFBS_SG3YC1 within the genus *Nemania*. Bootstrap values (>50%) from 1,000 replicates are shown above the branches. The tree was rooted using *Hypoxylon pulicicidum* (JX183075) as outgroup. Scale bar represents 0.08 substitutions per site.

Phylogenetic analysis based on ITS sequences placed isolates USTFBS_SG5MC5 and USTFBS_SG2YA2 within the *Fusarium incarnatum–equiseti* species complex (FIESC). Both grouped with *F. equiseti* reference strains (MH862468, GQ505688, NR_121457) with moderate support, consistent with their affiliation to the *Equiseti* lineage of FIESC (Fig. 8). Non-FIESC species (*F. guilinense*, *F. citri*, *F. hainanense*, *F. pernambucanum*) formed distinct, well-supported clades, confirming the monophyly and clear separation of the FIESC cluster.

However, the internal branches within FIESC exhibited low bootstrap support, reflecting the known limitation of the ITS region in resolving cryptic *Fusarium* species. The ITS locus is generally too conserved to discriminate between closely related taxa such as *F. equiseti*, *F. incarnatum*, and their phylogenetic species variants. Despite these limitations, the consistent clustering of both isolates with authenticated FIESC sequences provides reliable evidence of their genetic affiliation, sufficient for ecological and functional characterization within this complex.

The phylogenetic tree positions USTFBS SG5YD5 (in red) within the *Occultitheca–Clypeosphaeria* clade of the family Xylariaceae, indicating a close genetic relationship with *Occultitheca rosae*. Despite this affinity, SG5YD5 exhibits a distinct branch separation (bootstrap = 35) from the *O. rosae* clade, suggesting possible variation or an uncharacterized species-level divergence within *Occultitheca* (Fig. 9). Its intermediate placement between *O. ananasi* and *Clypeosphaeria mamillana* further supports the idea that this isolate represents a poorly resolved taxon within the *Occultitheca–Clypeosphaeria* complex. Regardless, this ITS phylogeny shows that the isolate USTFBS SG5YD5 is identified as *Occultitheca* sp., clustering within the *O. rosae* lineage but showing distinct divergence that warrants further taxonomic resolution.

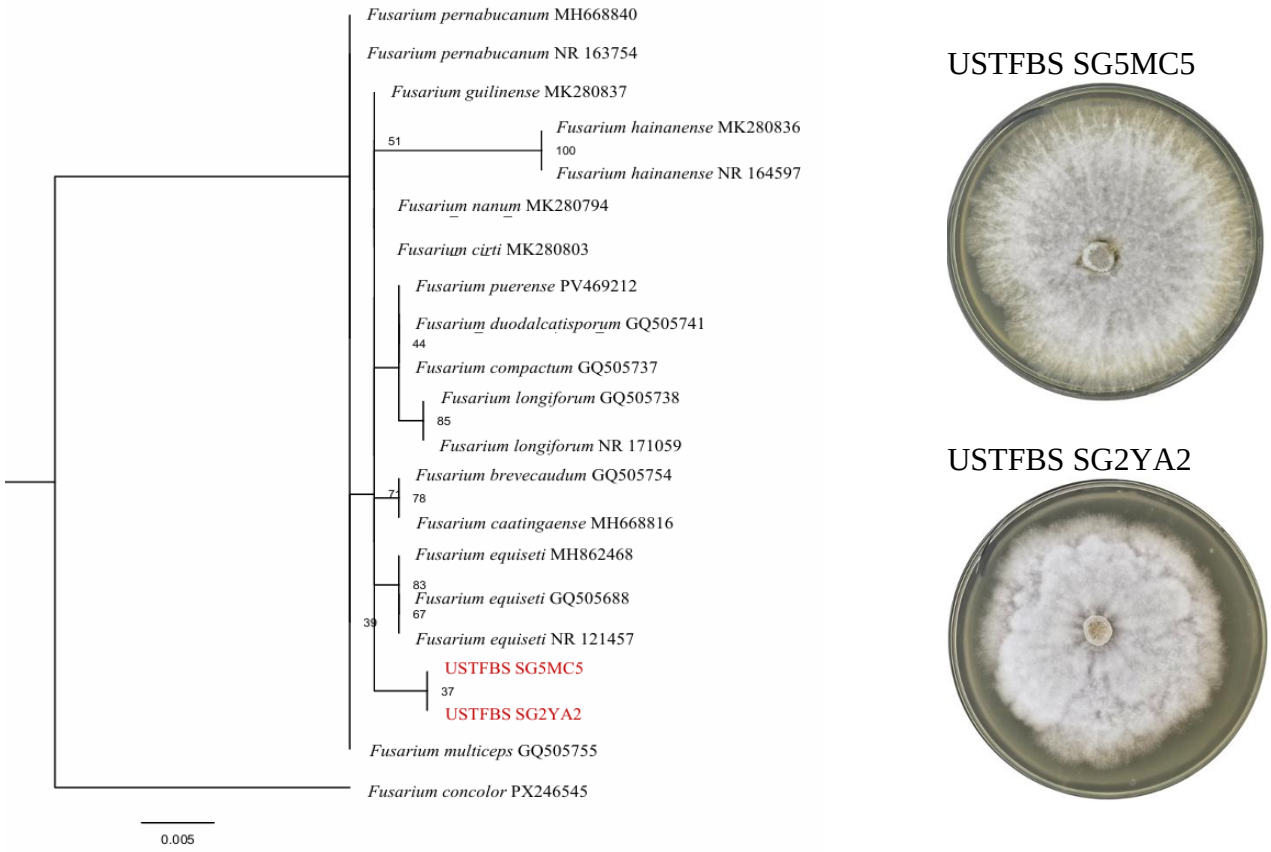

Fig. 8 – Maximum Likelihood phylogenetic tree based on ITS rDNA sequences showing the placement of isolate USTFBS SG5MC5 and SG2YA2 within the genus *Fusarium incarnatum-equiseti* complex. The tree was rooted using *Fusarium concolor* (PX246545) as outgroup. Scale bar represents 0.05 substitutions per site.

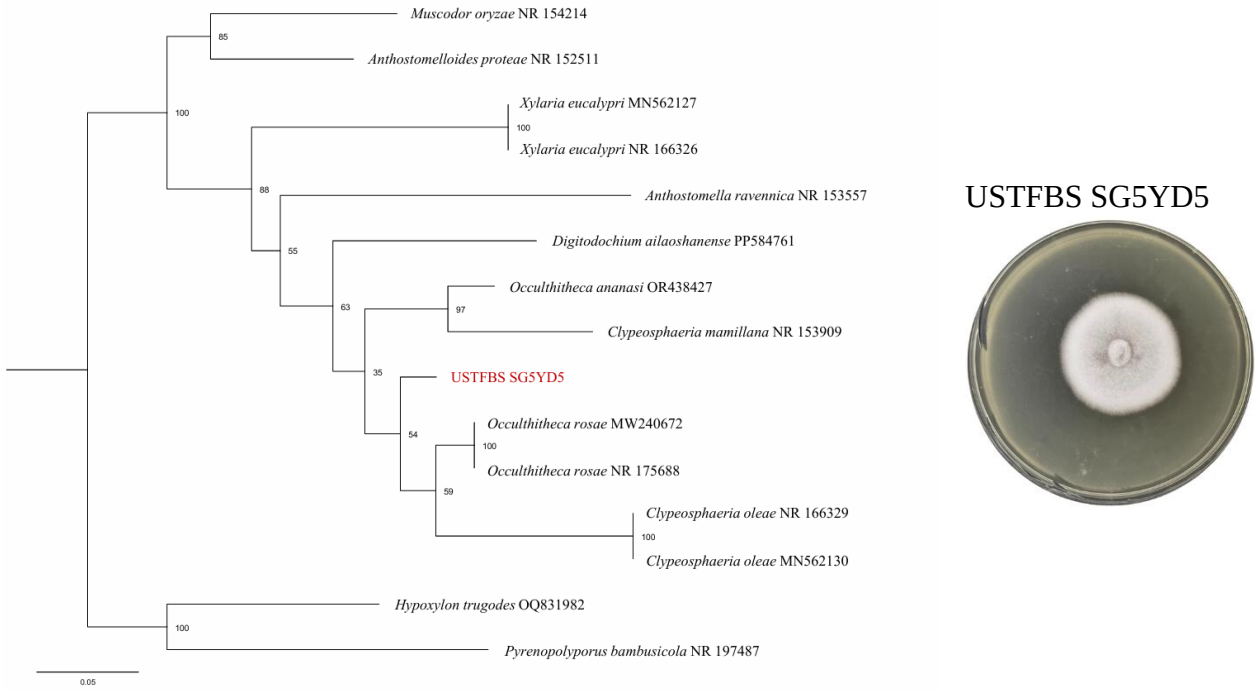

Fig. 9 – Phylogenetic affiliation of the unidentified endolichenic fungus USTFBS SG5YD5 within the Xylariaceae based on ITS rDNA sequences.

Discussion

Host Protection by Sagada-ELF

ELF are increasingly recognized for their ecological and biotechnological importance, yet studies on Philippine ELF remain limited. Reports have primarily focused on ELF from foliose lichens in lowland and montane habitats (Galinato et al. 2021, Santiago et al. 2021), revealing members of *Xylariaceae*, *Hypoxylaceae*, and *Trichocomaceae* as common associates. These taxa exhibit diverse metabolic capabilities, including secondary metabolite production and antagonism against phytopathogens (Chen et al. 2024, Guo et al. 2023). The present study expands this understanding by characterizing ELF associated with *Usnea* collected from Sagada, a high-elevation habitat with distinct microclimatic conditions (Santiago et al. 2021). The recovered isolates, belonging to *Xylaria*, *Nemania, Hypoxylon,* and *Fusarium*, reflect both cosmopolitan and potentially host-specific fungal taxa.

Dual-culture assays demonstrated that ELF from both young and mature ELF from *Usnea* thalli inhibited *Fusarium oxysporum*, indicating that antagonism is a conserved trait across developmental age or thallus type. Although mean inhibition values were comparable between groups, young-thallus Sagada-ELF isolates showed higher variability, with several (e.g., SG1YA1, SG3YA2) producing strong inhibition zones. We hypothesize that ELF from mature thalli may show heightened, more stable antifungal activity, reflecting traits expressed after prolonged colonization and defense establishment. Similar patterns are supported by studies showing (i) strong antagonism by endophytes isolated from *Sesuvium portulacastrum* (Karunasinghe et al. 2020) and from *Camellia reticulata* tissues (Huang et al. 2024), and (ii) host developmental stage (young vs. mature leaves) shaping endophyte community composition and antipathogen functions (Castillo-González et al. 2025). The study of Yang et al. (2021) highly supports this and stated that thallus age alters recovery and diversity of ELF from *Parmotrema tinctorum*, implying that age is a real axis affecting ELF.

Type B (mutual inhibition upon contact) predominated, accounting for 55% of interactions in mature thalli and 35% in young thalli. This pattern suggests ELF–pathogen recognition via surface contact, mechanisms previously described in antagonistic fungi such as *Trichoderma* and *Penicillium* as contact-inhibition phenomena (Schirmböck et al. 1994). In such interactions, both mycelia cease growth at the point of contact, forming a visible boundary that reflects activation of cell-wall-degrading enzymes or secondary metabolite production to maintain territorial integrity (Liu et al. 2023). The prevalence of such mutual inhibition among the thallus ELF implies that contact-based antagonism may be a regulated, stabilized defense strategy within established lichen communities.

In our data, Type D interactions (inhibition upon contact) were more frequent among young ELF, while mature ELF showed a higher incidence of Type E (distance inhibition). This pattern may reflect a shift from resource-driven, direct contact competition toward diffusible/volatile metabolite–mediated antagonism. Similar mechanisms (volatile/non-volatile metabolite production) have been documented in antagonistic fungi such as *Trichoderma* spp. (Vinale et al. 2008) and known producers of cytochalasin/polyketide metabolites such as *Xylaria* spp. (Tan et al. 2024).

Potent inhibition observed in *Nemania* and *Xylaria* isolates reinforces their biocontrol potential. These genera are known to synthesize polyketides, cytochalasins, and volatile compounds with strong antifungal effects (Galinato et al. 2021, Santiago et al. 2021). In particular, *Xylaria* species which were isolated as endophytes or ELF, are known to secrete diverse polyketides and cytochalasin derivatives with broad-spectrum antimicrobial activity (Chomnunti et al. 2014, Tan et al. 2024). *Nemania* species likewise produce volatile and soluble metabolites which were implicated in pathogen suppression and inter-fungal antagonism (Zhang et al. 2023). The presence of all five interaction types across both thallus ages suggests a functional continuum between competition and coexistence, where ELF contributes to maintaining microbial balance within the lichen and potentially offers protection against plant pathogens.

Growth promoting properties of Sagada-ELF

Several previous studies show that fungal endophytes can produce IAA in *vitro* in values in the range of 3–30 µg/mL (Turbat et al. 2020, García-Latorre et al. 2023). The study of de Souza Silva et

al. (2025) demonstrated that filamentous fungi isolated from Antarctic lichens and sediments, particularly *Cladosporium* sp., can effectively solubilize inorganic phosphates under cold, saline, and alkaline conditions; thus, revealing novel cold-adapted microbial candidates for sustainable phosphorus mobilization. In this study, IAA production was observed in both young and mature isolates, with peak levels (>40 µg/mL) recorded for *Xylaria laevis* (SG4MB5.2) and *Xylaria enteroleuca* (SG5MB3.1). Because fungal IAA synthesis is typically tryptophan-dependent via indole-3-pyruvate or tryptamine pathways, its production likely supports not only plant root stimulation (Tsavkelova et al. 2012) but also internal lichen morphogenesis and partner signaling.

The co-occurrence of IAA synthesis and phosphate solubilization implies synergistic nutrient-mobilizing and signaling capacities that could translate to host growth promotion. While no significant difference in mean IAA or phosphate solubilization was observed between thallus ages, individual variability was notable. This indicates that ELF potential is primarily species-driven rather than stage-dependent. *Fusarium* isolates (e.g., SG1YB4, SG2YA2) exhibited lower IAA output, consistent with their competitive or pathogenic tendencies, whereas *Xylaria* ELF displayed better activities. Such taxonomic trends emphasize that ELF metabolic versatility is largely intrinsic to their lineage, though modulated by the lichen's developmental stage.

These beneficial traits of ELF reflect both inherited potential (species specificity) and environmental expression (phenotypic plasticity). The *Usnea* thallus provides a stable yet dynamic scaffold where nutrient availability and chemical gradients shift as the lichen matures. Young thalli, characterized by rapid growth and limited metabolites, promotes more variable and competitive ELF behavior which was manifested in this study as higher antagonistic variability and direct inhibition. Mature thalli, in contrast, favor regulated, chemically mediated interactions and nutrient mobilization through phosphate solubilization and stable IAA synthesis. Such stability ensures that ELF communities collectively maintain the resilience of the lichen holobiont, balancing defense, nutrient cycling, and communication within their microecosystem.

The beneficial traits observed among Sagada-ELF, particularly *Xylaria* and *Nemania* species exhibiting strong antagonism, high IAA synthesis, and efficient phosphate solubilization, positions them as promising bioinoculants. These traits mirror those of established plant-beneficial fungi yet originate from symbiotic lineages adapted to extreme, nutrient-poor environments. Harnessing ELF could therefore contribute to eco-friendly agricultural strategies by improving nutrient uptake, enhancing crop resilience under stress, and reducing reliance on chemical fertilizers and pesticides. Future studies integrating metabolomic profiling, genomic analysis, and in *vivo* plant trials are recommended to elucidate underlying pathways and evaluate their practical application in sustainable crop management.

In summary, ELF from both young and mature *Usnea* thalli share a conserved suite of protective and growth-promoting traits whose expression varies with host developmental stage. Their capacity to inhibit pathogens and facilitate nutrient mobilization underscores their ecological versatility and biotechnological potential, bridging the functional continuum between lichen symbiosis and plant mutualism. The beneficial traits observed among Sagada-ELF, particularly *Xylaria*, *Hyphopichia*, and *Nemania* species exhibiting strong antagonism, high IAA production, and efficient phosphate solubilization, position them as promising bioinoculant candidates. This highlights their ecological role in maintaining lichen holobiont stability and resilience. These traits mirror those of established plant beneficial fungi yet originate from symbiotic lineages adapted to extreme, nutrient-poor environments. Thus, the metabolic versatility and biocontrol potential of Sagada-ELF position them as promising candidates for sustainable agriculture, offering eco-friendly strategies for pathogen suppression, nutrient mobilization, and plant growth enhancement. Future research integrating metabolomics, genomics, and plant-based trials will be crucial to translating these symbiotic adaptations into applied biotechnological solutions.

Acknowledgements

This research is supported by the DOST-NRCP Project No. E-261 – Project ELFHA: Biodiscovery of Endolichenic Fungi to mitigate antimicrobial resistance in Health and Agriculture.

The authors also acknowledge the UST Research Center for the Natural and Applied Sciences for additional research funding and thank Mr. Ghimel P. Espinosa for his valuable assistance in the isolation of endolichenic fungi under Project ELFHA. RJO Co further extend her heartfelt thanks to the DOST–Science Education Institute–Accelerated Science and Technology Human Resource Development Program for the graduate scholarship and thesis support. The authors also acknowledge the local government of Sagada, Mountain Province, particularly Hon. Mayor Felicito O. Dula, for giving us permission to collect our lichen hosts.

References

Castillo-González H, Slot JC, Yarwood S, Chaverri P et al. 2025 – Exploring Rubiaceae fungal endophytes across contrasting tropical forests, tree tissues, and developmental stages. Peer Community Journal 5, e26. Doi 10.24072/pcjournal.526

Chen W, Yu M, Chen S, Gong T et al. 2024 – Structures and biological activities of secondary metabolites from *Xylaria* spp. Journal of Fungi, 10(3), 190. Doi 10.3390/jof10030190

Chomnunti P, Hongsanan S, Hyde KD. 2014 – Diversity of Xylariaceous endophytes and their secondary metabolites. Fungal Diversity 66(1), 1–14. Doi 10.1007/s13225-014-0285-2

CodonCode Corporation. 2023 – CodonCode Aligner (Version 9.0.1) [Computer software]. CodonCode Corporation. https://codoncode.com/

Cruz EM, dela Cruz TEE. 2024 – Plant growth-promoting and protective potential of root fungal endophytes associated with a pioneer grass, *Saccharum spontaneum* L., from a lahar-affected area. Asian Journal of Mycology 7(2), 132–147. Doi 10.5943/ajom/7/2/9

de Souza Silva AV, Cury JC, de Souza Silva CM. 2025 – Phosphate solubilization by filamentous fungi from Antarctic lichens and sediments. Extremophiles 29(1), 26. Doi 10.1007/s00792-025-01396-0

dela Cruz TEE, Behr JH, Geistlinger J, Grosch R et al. 2023 – Monitoring of an applied beneficial *Trichoderma* strain in root-associated soil of field-grown maize by MALDI-TOF MS. Microorganisms 11, 1655. Doi 10.3390/microorganisms11071655

Galinato MGM, Bungihan ME, Santiago KAA, Sangvichien Eet al. 2021 – Antioxidant activities of fungi inhabiting *Ramalina peruviana*: insights on the role of endolichenic fungi in the lichen symbiosis. Current Research in Environmental & Applied Mycology (Journal of Fungal Biology) 11(1): 119-136.

García-Latorre C, Rodrigo S, Marin-Felix Y, Stadler M et al. 2023 – Plant-growth promoting activity of three fungal endophytes isolated from plants living in dehesas and their effect on *Lolium multiflorum*. Scientific Reports 13, 7354. Doi 10.1038/s41598-023-34036-8

Grimm M, Grube M, Schiefelbein U, Zühlke D et al. 2021 – The lichens' microbiota, still a mystery? Frontiers in Microbiology 12, 623839. Doi 10.3389/fmicb.2021.623839

Grube M, Cernava T, Soh J, Fuchs S et al. 2015 – Exploring functional contexts of symbiotic sustain within lichen-associated bacteria by comparative omics. The ISME Journal 9(2), 412–424. Doi 10.1038/ismej.2014.138

Guo Q, Shi L, Wang X, Li D et al. 2023 – Structures and biological activities of secondary metabolites from the *Trichoderma* genus (covering 2018–2022). Journal of Agricultural and Food Chemistry, 71(37), 13612-13632. Doi 10.1021/acs.jafc.3c04540

Guzmán-Guzmán P, Porras-Troncoso MD, Olmedo-Monfil V, Herrera-Estrella A. 2019 – *Trichoderma* species: Versatile plant symbionts. Phytopathology 109(1), 6–16. Doi 10.1094/phyto-07-18-0218-rvw

Huang R, Meng Q, Xun L, Wu X et al. 2024 – Antagonistic effects of endophytic fungi from *Camellia reticulata* pedicels on yeasts: Implications for antimicrobial mechanism of nectar. Frontiers in Plant Science 15, 1494855. Doi 10.3389/fpls.2024.1494855

Jamilano-Llames LC, dela Cruz TEE. 2025 – Comparative antagonistic activities of endolichenic fungi isolated from the fruticose lichens *Ramalina* and *Usnea*. Journal of Fungi 11(4), 302. Doi 10.3390/jof11040302

Karunasinghe TG, Maharachchikumbura SSN, Velazhahan R, Al-Sadi AM. 2020 – Antagonistic activity of endophytic and rhizosphere fungi isolated from sea purslane (*Sesuvium portulacastrum*) against *Pythium* damping-off of cucumber. Plant Disease 104(10), 2670–2677. Doi 10.1094/PDIS-01-20-0003-RE

Kellogg JJ, Raja HA. 2017 – Endolichenic fungi: A new source of rich bioactive secondary metabolites on the horizon. Phytochemical Reviews 16, 271–293. Doi 10.1007/s11101-016-9473-1

Lemoine F, Correia D, Lefort V, Doppelt-Azeroual O et al. 2019 – NGPhylogeny.fr: new generation phylogenetic services for non-specialists. Nucleic Acids Research 47(W1), W260–W265. Doi 10.1093/nar/gkz303

Li Y, Huang Y, Wronski T, Huang M. 2023 – Diversity of bacteria associated with lichens in Mt. Yunmeng in Beijing, China. PeerJ. Doi 10.7717/peerj.16442

Li Y, Kromer B, Schukraft G, Bubenzer O et al. 2014 – Growth rate of *Usnea aurantiacoatra* (Jacq.) Bory on Fildes Peninsula, Antarctica and its climatic background. PLoS One 9(6), e100735. Doi 10.1371/journal.pone.0100735

Liu Y, Chen J, Zhang X. 2023 – Antagonistic fungi and their inhibitory effects on plant pathogens: Dual culture evidence. Frontiers in Microbiology 14, 10187083. Doi 10.3389/fmicb.2023.10187083

Miller MA, Pfeiffer W, Schwartz T. 2011 – The CIPRES Science Gateway: a community resource for phylogenetic analyses. Proceedings of the 2011 TeraGrid Conference: Extreme Digital Discovery, 1–8. Doi 10.1145/2016741.2016785

Paguirigan JAG, dela Cruz TEE, Santiago KAA, Gerlach A et al. 2020 – A checklist of lichens known from the Philippines. Current Research in Environmental and Applied Mycology, 10(1), 319-376. Doi 10.5943/CREAM/10/1/29

Rambaut A. 2009 – FigTree: tree figure drawing tool. Institute of Evolutionary Biology, University of Edinburgh. http://tree.bio.ed.ac.uk/software/figtree

Sachdeva G, Das A. 2022 – Communication between immune system and mycobiota impacts health and disease. Proceedings of the Indian National Science Academy, 88(3), 250–262. doi: 10.1007/s43538-022-00082-5.

Santiago KAA, dela Cruz TEE, Ting A. 2021 – Diversity and bioactivity of endolichenic fungi in *Usnea* lichens of the Philippines. Czech Mycology 73(1): 1-19. http://czechmycology.org/doi/doi-cmy.php?a=73101

Schirmböck M, Lorito M, Wang YL, Hayes CK et al. 1994 – Parallel formation and synergism of hydrolytic enzymes and peptaibol antibiotics in *Trichoderma harzianum*. Applied and Environmental Microbiology 60(12), 4364–4370.

Schouteden N, De Waele D, Panis B, Vos CM. 2015 – Arbuscular mycorrhizal fungi for the biocontrol of plant-parasitic nematodes: A review of the mechanisms involved. Frontiers in Microbiology 6, 1280. Doi 10.3389/fmicb.2015.01280

Suryanarayanan TS, Thirunavukkarasu N. 2017 – Endolichenic fungi: The lesser-known fungal associates of lichens. Mycology 8(3), 189–196. Doi 10.1080/21501203.2017.1352048

Taer EC, Dal-Forno M, Moncada B, Amoroso VB et al. 2023 – Lichens across land use types of Mt. Musuan, Bukidnon, Southern Philippines. Philippine Journal of Science 152(6A), 2077–2086. https://ukdr.uplb.edu.ph/journal-articles/6231

Tan MA, Castro SG, Oliva PMP, Yap PRJ et al. 2020 – Biodiscovery of antibacterial constituents from the endolichenic fungi isolated from *Parmotrema rampoddense*. 3 Biotech 10(5), 212. Doi 10.1007/s13205-020-02213

Tan MA, dela Cruz JD, Magpantay HD, Apurillo CCS et al. 2024 – Isolation of griseofulvin from the endolichenic fungus *Cubamyces menziesii* (Berk.) Lücking inhabiting *Parmotrema rampoddense* (Nyl.) Hale. Science & Engineering Journal 17 (Supplement), 432. Doi 10.54645/202417SupKXN-49

Tan Q, Ye X, Fu S, Yin Y et al. 2024 – The cytochalasins and polyketides from a mangrove endophytic fungus *Xylaria arbuscula* QYF. Marine Drugs, 22(9), 407. doi: 10.3390/md22090407.

Treseder KK, Lennon JT. 2015 – Fungal traits that drive ecosystem dynamics on land. Microbiology and Molecular Biology Reviews 79(2), 243–262. Doi 10.1128/MMBR.00001-15

Tsavkelova EA, Klimova SY, Cherdyntseva TA, Netrusov AI. 2012 – Microbial producers of plant growth stimulators and their practical use: A review. Applied Biochemistry and Microbiology 48(1), 1–11. Doi 10.1134/S0003683812010163

Turbat A, Pandey R, Sahoo D. 2020 – Production of indole-3-acetic acid (IAA) by endophytic fungi isolated from medicinal plants and its effect on plant growth. Journal of Applied Biology & Biotechnology 8(2), 53–59. Doi 10.7324/JABB.2020.80209

U'Ren JM, Lutzoni F, Miadlikowska J, Laetsch AD et al. 2012 – Host and geographic structure of endophytic and endolichenic fungi at a continental scale. American Journal of Botany 99(5), 898–914. Doi 10.3732/ajb.1100459

Underhill DM, Iliev ID. 2014 – The mycobiota: Interactions between commensal fungi and the host immune system. Nature Reviews Immunology 14(6), 405–416. Doi 10.1038/nri3684

Vinale F, Sivasithamparam K, Ghisalberti EL, Woo SL et al. 2008 – *Trichoderma*–plant–pathogen interactions. Soil Biology and Biochemistry 40(1), 1–10.

Wang Q, Li J, Yang J, Zou Y et al. 2022 – Diversity of endophytic bacterial and fungal microbiota associated with the medicinal lichen *Usnea longissimi* at high altitudes. Front. Microbiol. 13:958917. Doi 10.3389/fmicb.2022.958917

Wicklow DT. 1975 – Interference competition and the organization of fungal communities. In The Fungal Community: Its Organization and Role in the Ecosystem, 265–282.

Yang JH, Oh S-Y, Kim W, Woo J-J et al. 2021 – Effect of isolation conditions (including thallus age) on the diversity of endolichenic fungi from *Parmotrema tinctorum*. Journal of Fungi 7(5), 335. https://doi.org/10.3390/jof7050335

Zhang Y, Ma S, Xu L. 2023 – Bioactive metabolites from *Nemania* spp.: Structures, activities, and biosynthesis. Journal of Fungi 9(8), 815 Doi 10.3390/jof9080815

Zhang W, Ran Q, Li H, Lou H. 2024 – Endolichenic fungi: A promising medicinal microbial resource to discover bioactive natural molecules - An update. Journal of Fungi, 10(2), 99. https://doi.org/10.3390/jof10020099